Numerical Modeling of Space Plasma Flows: Astronum-2006
ASP Conference Series, Vol. 359, 2006
Pogorelov, Nikolai V.; Zank, Gary P.

Front Tracking under TSTT

James Glimm, Brian Fix, Xiaolin Li, Jinjie Liu and Xinfeng Liu

Department of Applied Mathematics and Statistics, University at Stony Brook, Stony Brook, NY 11794–3600

Tianshi Lu, Roman Samulyak and Zhiliang Xu

Computational Science Center, Brookhaven National Laboratory, Upton, NY 11973

Abstract. We report several important developments of the front tracking method and applications in science and engineering under the TSTT project. The progress includes the extraction of an independent software library from the front tracking code, conservative front tracking, applications of front tracking to the simulation of fusion pellet injection in a magnetically confined plasma, the study of a fuel injection jet, and the study of fluid chaotic mixing, among other problems.

1. Introduction

The Center for Terascale Simulation Tools and Technology (TSTT) is DOE sponsored as part of its Scientific Discovery through Advanced Computing (SciDAC) program. The objective of this center is to facilitate the use of advanced mesh tools for increasingly complex, realistic simulations of PDE-based applications. Numerous software tools are available to help manage the complexity of these simulations, including computer-aided design systems used to represent the geometry of the computational domain, mesh generation tools to discretize those domains, solution adaptive methods (AMR) to improve the accuracy and efficiency of simulation techniques, tools for tracking a dynamically moving front, and parallel tools such as dynamic partitioning to ease implementation on today's computer architectures. These tools would be particularly effective if they could be easily integrated and used in concert in existing simulations, or if they could enable integration of existing simulations into multi-physics, multi-scale application problems. At present, however, this type of integration is exceedingly difficult, largely due to software compatibility issues rather than to the underlying technical issues.

Numerical simulations can be performed more efficiently using the latest technologies. The TSTT Center has developed interoperable and interchangeable mesh, geometry, and field manipulation tools that are of direct use to the DOE SciDAC applications. The premise of our technology development is that advanced mesh, geometry and field services can be provided as libraries that can be used with minimal intrusion into application codes. During SciDAC-1, the TSTT team developed and deployed a number of advanced technologies — including the *Frontier-Lite* front tracking library of Fix et al. (2005), the

Mesquite mesh quality improvement toolkit of Brewer et al. (2003), and unstructured mesh refinement of Shephard et al. (2005) and mesh swapping tools — that provide ample evidence of the viability of this approach. Moreover, we combined these *component services* in an interoperable manner to provide new *integrated services* such as AMR-front tracking, parallel adaptive loop libraries, and combined geometry-mesh modification tools for use in shape optimization applications. Critical to the TSTT interoperability goal is the development of common interfaces that provide data-structure-neutral access to mesh, geometry, and field information. These interfaces provide access to all TSTT services in a uniform way and are fundamental to creating interoperability for the integrated services. Moreover, a uniform interface allows easier experimentation with different, but functionally similar, technologies to determine which is best suited for a given application. The development of such interfaces requires creating a consensus among a large group of mesh, geometry, and field experts. This is a difficult technical and sociological challenge that would have been impossible without the collaborative environment fostered by the SciDAC program. It is this integration of a wide range of DOE and university mesh-related technologies under a common interface that distinguishes TSTT as a center.

In this paper, we introduce several applications of the TSTT tools to SciDAC applications conducted at SUNY Stony Brook and Brookhaven National Laboratory.

2. FronTier-Lite, An Software Library for Interface Tracking

A general purpose software package for the geometry and dynamics of an interface has been extracted from the FronTier code developed by the authors and colleagues. The code is downloadable from the web, and is accompanied by a web based testing and evaluation site as well as a web based documentation. We describe significant improvements to this Front Tracking package, especially in the 3D handling of topological bifurcations.

A major new algorithm called Locally Grid Based tracking (LGB), which combines the best features of two previous 3D tracking algorithms is introduced in this software package. It combines the robustness of grid based tracking with the accuracy of grid free tracking, and thus it is a significant improvement to both of these algorithms.

We assess the performance of the package, in comparison with publicly distributed interface codes (the level set method), with published performance results (volume of fluid (VOF) and other methods) and with previous versions of front tracking. In comparison with the level set method, we used the fifth order WENO scheme for the convection of the level set function, while for the front tracking code, we used the fourth order Runge-Kutta method for the point propagation. Benchmark cases include the rotation of a slotted disk and an ellipse moving in a swirling velocity field. In both of these tests, the front tracking showed enduring correctness of the front topology and resolution while the level set broke down at an early time. Figure 1 shows a comparison test for a rotating slotted disk.

In comparison with the VOF method, we have applied the deformation velocity field acting on a sphere. The front tracking code gives a solution superior

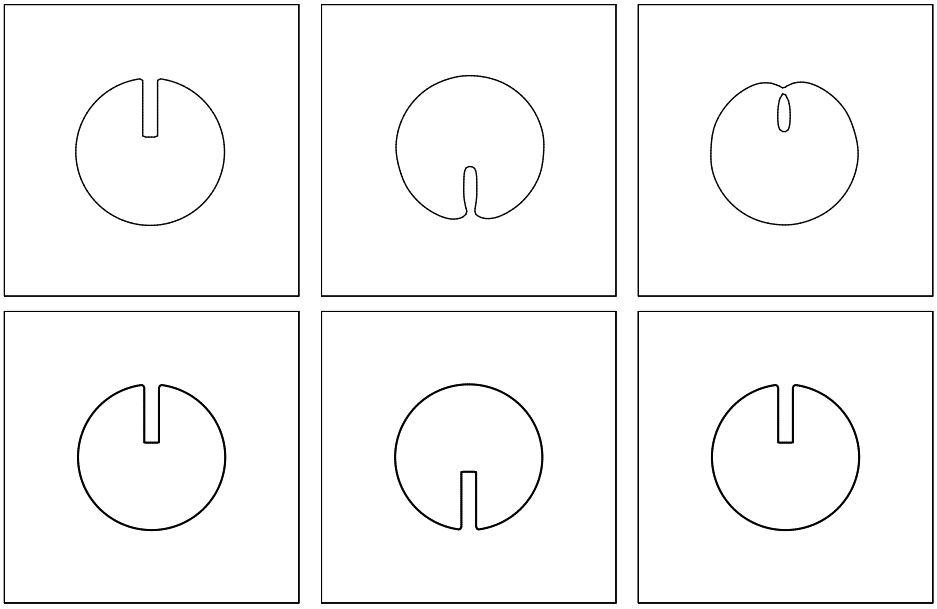

Figure 1. Comparison of slotted disk simulation using high order methods. The upper sequence shows the result of the level set method using the fifth order WENO scheme and the lower sequence shows the result of front tracking using the fourth order Runge-Kutta method.

both qualitatively and quantitatively to that of the VOF method, especially when the interface is stretched to become narrow and thin, Du et al. (2006).

3. Conservative Front Tracking

Conservative front tracking increases the order of convergence for the truncation error at a discontinuity and therefore converges to the physical solution faster than ordinary tracking or untracked algorithms. We have implemented a fully conservative front tracking algorithm for an N-dimensional system of nonlinear conservation laws.

The new algorithm is based on the divergence form of the conservation law in a space-time domain. Consider a system of conservation laws in N spatial dimension in differential form

$$\frac{\partial U}{\partial t} + \nabla \cdot F(U) = 0, \quad F = (f_1, f_2, ..., f_N) \quad , \tag{1}$$

where $U \in \mathbf{R}^p$ and $f_j(U) = (f_{1j}(U), ..., f_{pj}(U))^T \in \mathbf{R}^p$ are defined in a spatial domain $\Omega \subset \mathbf{R}^N$.

Integrating (1) in a time-space domain $\mathcal{V} \subset \mathbf{R}^{N+1}$, we obtain the integral form of (1),

$$\int_{\mathcal{V}} (\frac{\partial U}{\partial t} + \nabla \cdot F(U)) d\mathcal{V} = 0 \; . \tag{2}$$

By the divergence theorem, we have

$$\int_{\partial \mathcal{V}} (U, F(U)) \cdot \mathbf{n} dS = 0 \ . \tag{3}$$

The finite difference method presented here is an explicit finite volume integration scheme based on the integral form (3).

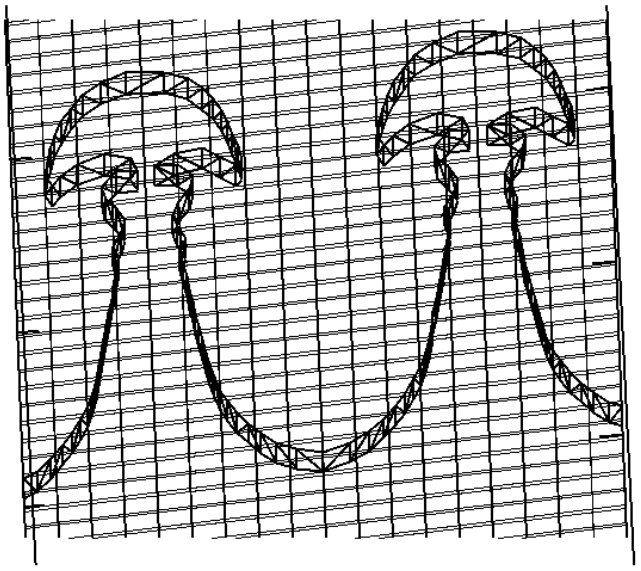

Figure 2. An example of 3D space-time interfaces joining two sequential time steps.

Assume a space-time discretization $\{\mathcal{V}_i\}$ which conforms to the space-time interface (see Figure 2) as U evolves in one time step from t_n to t_{n+1}. We solve (3) explicitly in this region. We define each $\mathcal{V}_i$ as a space-time control volume, and $\partial \mathcal{V}_i = D_i^n \cup D_i^{n+1} \cup \hat{S}_i$ with D_i^n, D_i^{n+1}, and $\hat{S}_i$ meeting at most at their boundaries. Here D_i^n and D_i^{n+1} are the boundary surfaces of $\mathcal{V}_i$ at time level n and $n+1$ respectively, and $\hat{S}_i$ is the complementary boundary surface of $\mathcal{V}_i$. Dividing the calculation of the integral (3) into three parts over D_i^n, D_i^{n+1} and $\hat{S}_i$ respectively, we have

$$|D_i^{n+1}| \ \overline{U}_i^{n+1} = |D_i^n| \ \overline{U}_i^n - \int_{\hat{S}_i} (U, F(U)) \cdot \mathbf{n} dS \ , \tag{4}$$

where

$$\overline{U}_i^n = \frac{1}{|D_i^n|} \int_{D_i^n} U(x_1, ..., x_N, t_n) dx_1 ... dx_N$$

and

$$\overline{U}_i^{n+1} = \frac{1}{|D_i^{n+1}|} \int_{D_i^{n+1}} U(x_1, ..., x_N, t_{n+1}) dx_1 ... dx_N$$

are cell averages, $|D_i^n|$ is the face area of D_i^n, $|D_i^{n+1}|$ is the face area of D_i^{n+1}, and $\mathbf{n}$ is the outward normal of $\hat{S}_i$. Therefore, $\overline{U}_i^{n+1}$, is the solution to (4) at time t_{n+1}.

To calculate $\overline{U}_i^{n+1}$, we first need to determine the space-time control volume $\{\mathcal{V}_i\}$. Then we calculate the fluxes defined on the surfaces of $\mathcal{V}_i$, so that we can apply (4).

4. Fuel Injection for the ITER

The injection of frozen pellets of deuterium and tritium is considered the major mechanism for refueling of the Tokamak nuclear fusion reactors. This problem is significantly important for the International Thermonuclear Experimental Reactor (ITER). However, challenging problems remain to be solved before achieving accurate numerical simulations of pellet ablation. The required level of detail in modeling is not available in standard MHD codes for fusion plasmas. Qualitatively new simulations are also required to estimate the efficiency of the recently proposed methods of laser ablation (rocket) and gyrotron driven pellet acceleration. If successful, these methods will achieve pellet velocities of the order of kilometers per second, and deposit the pellet material deeply into the plasma in ITER. The goal of our work is to develop mathematical models and numerical algorithms, and perform numerical simulations of processes associated with the injection of frozen deuterium-tritium fuel pellets in the tokamak. TSTT Front Tracking technology is a critical part of our computational model for tokamak fueling.

We have developed a 2D axisymmetric model for pellet ablation in the tokamak based on the front tracking MHD code for low magnetic Reynolds number free surface flows Samulyak & Prykarpatskyy (2004). The system of MHD equations in the low magnetic Reynolds number approximation is a coupled hyperbolic-elliptic system in geometrically complex moving domain:

$$\frac{\partial \rho}{\partial t} = -\nabla \cdot (\rho \mathbf{v}), \tag{5}$$

$$\rho \left(\frac{\partial}{\partial t} + \mathbf{v} \cdot \nabla \right) \mathbf{v} = -\nabla P + \mathbf{J} \times \mathbf{B}, \tag{6}$$

$$\rho \left(\frac{\partial}{\partial t} + \mathbf{v} \cdot \nabla \right) e = -P \nabla \cdot \mathbf{v} + \frac{1}{\sigma} \mathbf{J}^2 - \nabla \cdot \mathbf{q}, \tag{7}$$

$$\nabla \cdot \sigma \nabla \phi = \nabla \cdot \sigma (\mathbf{v} \times \mathbf{B}), \quad \left. \frac{\partial \phi}{\partial \mathbf{n}} \right|_{\Gamma} = (\mathbf{v} \times \mathbf{B}) \cdot \mathbf{n}, \tag{8}$$

$$P = P(\rho, e), \quad \mathbf{J} = \sigma \left(-\nabla \phi + \mathbf{v} \times \mathbf{B} \right). \tag{9}$$

Here $\mathbf{v}$, ρ and e are the velocity, density and the specific internal energy of the fluid, respectively, P is the pressure, $\mathbf{B}$ is the magnetic field induction, $\mathbf{J}$ is the current density distribution, σ is the fluid conductivity, and ϕ is the electric field potential, satisfying the Poisson equation with Neumann boundary condition (8). An external heat source $-\nabla \cdot \mathbf{q}$ represents the electron heat flux in the pellet ablation problem.

We have developed a numerical method for solving such a system and corresponding parallel software. In an operator splitting approach, we solve the

hyperbolic subsystem (5) - (7) using the hydrodynamic package of the FronTier code. The elliptic problem (8) is solved using either a mixed finite element discretization on a triangular (tetrahedral) mesh dynamically conforming to the moving interface, or the embedded boundary discretization Johansen & Colella (1998) on the rectangular mesh. The embedded boundary method is based on the finite volume discretization in rectangular grid cells, and irregular cells adjacent to the interface. The irregular domain is embedded in the rectangular Cartesian grid, and the solution is treated as a cell-centered quantity, even when these centers are outside of the domain. This ensures that the conditioning of fluxes is relatively unaffected by small cell volumes. The conservative second order accurate fluxes are calculated on every irregular cell boundary. The method fits very naturally to the internal structure of the FronTier code since one of its major interface propagation algorithms, the grid based tracking Du et al. (2006), explicitly constructs irregular cells adjacent to the interface. The implementation of elliptic solvers in the FronTier code can be beneficial not only to MHD. It can also enable the explicit treatment of viscosity for highly viscous fluids (when the explicit inclusion of the parabolic viscous terms limits the time step due to the Courant-Friedrichs-Lewy (CFL) stability condition), and the incompressible formulation of the fluid dynamics equations within Chorin's projection method, both for multifluid problems with discontinuity interfaces. The linear systems resulting from the embedded boundary discretization are solved using parallel iterative solvers, including algebraic multigrid (AMG), and preconditioners implemented in PETSC Balay et al. (2001) and Hypre packages.

Since the method of front tracking allows the study of multiphysics phenomena in multiphase systems characterized by strong discontinuities in physical properties of the system components, it is ideally suitable to the pellet ablation problem. In our computational model, explicit interfaces separate the solid pellet from the ablated gas, and the cold, dense, and weakly ionized ablation cloud from the highly conducting fusion plasma. Realistic equations of state are employed in different geometrical regions corresponding to different states of matter. The code is capable of simulating the transition of deuterium in the pellet from a solid to a vapor state under high ablation pressures. A surface ablation model is used on the pellet surface. An electronic heat flux model for the calculation of the thermal energy deposition in the ablation cloud and on the pellet surface uses analytical approximations to the solution of the kinetic equation Ishizaki et al. (2004). Atomic physics processes in the ablation cloud such as dissociation, recombination, and ionization are taken into account by the EOS model for weakly ionized plasmas. Using this model, we have performed studies of the pellet ablation physics, pellet ablation rate and the lifetime in the magnetic field, and compared with analytical predictions and previous numerical simulations. The 1D version of the model is in excellent agreement with the scaling laws and ablation rate predicted by the NGS model Parks & Turnbull (1978). The 2D axisymmetric simulations agree with results of MacAulay (1994), and Ishizaki et al. (2004). Our work goes beyond these studies and calculates properties of the ablation channel in magnetic fields. Shapes of the ablation cloud at early time in magnetic fields ranging from 0 to 5 Tesla are depicted in Figure 3. For the first time, we have performed simulations leading to the calculation of ablation rates in magnetic fields Samulyak et al. (2006).

In the future, we will use a 3D model of the pellet ablation for the study of striation instabilities. These instabilities are presently not well understood.

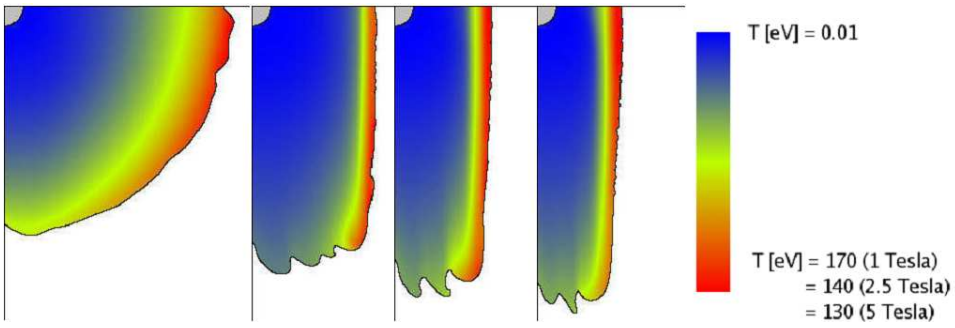

Figure 3. FronTier simulation of the formation of pellet ablation channels in magnetic fields ranging from 0 (left) to 5 Tesla (right). Temperature distributions are shown.

5. Turbulent Mixing

Turbulent mixing of acceleration driven fluids causes potential degradation of the performance of an ICF capsule. Acceleration by a steady driving force, known as the Rayleigh-Taylor mixing problem, is a specific and prototypical special case. Until recently, most simulation codes disagreed with experimental measurements for even the most basic diagnostic, the overall mixing rate, by a factor of two. Several explanations have been offered for this fact, the one we favor being that the simulations are hampered by excess numerical mass diffusion and insufficient physics models.

Using TSTT developed front tracking software, we cured the first problem, excess numerical mass diffusion, and by enhancements to this software, we also address the second problem, insufficient physics models for physical mass diffusion and/or physical surface tension, see Liu et al. (2006). The result is complete agreement or nearly so in the match of simulation to experiment for Rayleigh-Taylor mixing.

6. Diesel Fuel Injection and Jet Atomization

We have studied the cavitation and atomization of high speed liquid jets in combustion applications. In the design of a fuel injector, the characteristics of the spray are crucial variables to improve the engine performance and reduce the pollution. Despite substantial theoretical and experimental efforts, many of the atomization mechanisms remain untested and the mechanisms of atomization are still a research issue. Thus, direct numerical simulations are critical for improving spray predictions, understanding atomization mechanisms and providing input to spray combustion models for predictive modeling of diesel engine combustion.

We have studied the influence of cavitation on the spray formation. The phase transition is governed by the compressible Euler equations with heat dif-

fusion. The phase boundary in one dimension is modeled as a tracked interface

$$\frac{\partial U}{\partial t} + \frac{\partial F(U)}{\partial x} = 0, \tag{10}$$

where $U = [\rho, \rho u, \rho E]^\tau$, $F(U) = [\rho u, \rho u^2 + P, \rho u E + uP - \kappa \frac{\partial T}{\partial x}]^\tau$, ρ denotes density, u velocity, P pressure, $E = u^2/2 + \epsilon$ is the specific total energy, ϵ is the specific internal energy, κ is the coefficient of thermal diffusion, and T is temperature. Integrating the conservation equations (10) across the interface, we obtain the balance equations for the mass, momentum, and total energy, respectively:

$$[\rho u] = s[\rho] \ , \tag{11}$$

$$[\rho u^2 + P] = s[\rho u] \ , \tag{12}$$

$$[\rho u E + uP - \kappa \nabla T] = s[\rho E] \ , \tag{13}$$

where s is the interface velocity. We also postulate that the temperature is continuous across the phase boundary. Therefore, the interfacial temperatures of the vapor and liquid are equal

$$T_{\rm l} = T_{\rm v} = T_{\rm s} \ , \tag{14}$$

where $T_{\rm s}$ is the interface temperature. To complete the formulation we need to provide an equation relating the interface temperature $T_{\rm s}$ to the mass flux M. Denoting the equilibrium pressure at temperature T by $p_{\rm sat}(T)$, the net mass flux of evaporation is found from the kinetic theory

$$M = \alpha \frac{p_{\rm sat}(T) - p_{\rm v}}{\sqrt{2\pi R T}} \ . \tag{15}$$

We have developed an iterative phase boundary propagation algorithm. It generalizes the numerical methods for tracking the contact discontinuity of a Riemann problem, and introduces a subgrid model to account for the thin thermal layer around the phase boundary. In the phase boundary problem, velocities and pressures are discontinuous across the phase boundary, and satisfy the above interface conditions.

These numerical models have been used to simulate cavitation, jet breakup, and spray formation. The disturbance of the cavitation bubbles produced upstream significantly impact the downstream jet breakup. These vapor bubbles grow and break the jet surface, forming spray and droplets. For the details of the simulation and algorithms, see Xu et al. (2006) and Fig. 4.

7. Other Applications

We introduce briefly some other applications, led by or with important contributions from other institutions, under the TSTT Center:

- **Mesh Quality Improvement.** Development of the Mesquite toolkit Brewer et al. (2003) was initiated in SciDAC-1 to provide applications methods for post-processing or updating time-evolving meshes to improve

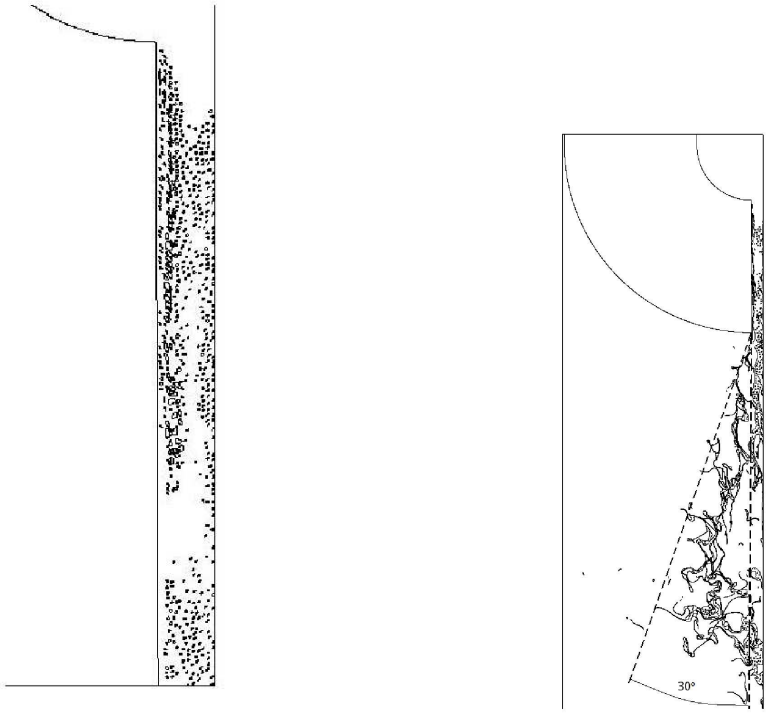

Figure 4. FronTier simulation of the liquid jet atomization. Left: mixed phase flow in nozzle. Right: atomization and spray.

structured, unstructured, and hybrid meshes. Key capabilities included mesh optimization for shape and size improvement, mesh validity guarantees, and methods for controlling meshes on deforming domains. Applications of Mesquite to scientific simulations include the accelerator optimization design, biology simulations, climate study, rocket propellant burn simulations, and fusion simulations.

- **AMR Front Tracking.** In SciDAC-1, TSTT researchers merged the front tracking code *FronTier-Lite* with the AMR code Overture to create a combined, AMR-front tracking capability needed by fusion, groundwater, combustion, and astrophysics applications. This code was created in 2D, although both components function in 2D and 3D.

- **Virtual Microbial Cell Simulator (VMCS).** TSTT mesh generation and discretization technologies were used in simulations that provided new scientific insight into the flocculation behavior of Shewanella microbes in oxygen rich environments by confirming that there is an oxygen gradient from the edges of the floc into the center Gorby (2004). This collaboration with PNNL computational biologists has resulted in the development of the VMCS Trease (2002) which is targeting DOE bioremediation problems in heavy metal waste.

Acknowledgements The authors of this work are supported in part by the National Science Foundation Grant DMS–0102480, the Army Research Office

Grant W911NF–05–1–0413, the U.S. Department of Energy Grant DE–AC02–98CH1-886, the U.S. Department of Energy Grant DE–FC02–01ER25461 and the U.S. Department of Energy Grant DE-AC028CH10886.

References

S. Balay, W. Gropp, L. McInnes, and B. Smith. Petsc users manual. Technical Report ANL-95/11 - Revision 2.1.1, 2001.

M. Brewer, L. Diachin, P. Knupp, T. Leurent, and D. Melander. The Mesquite mesh quality improvement toolkit. In *Proceedings of the 12th International Meshing Roundtable*, pages 239–250, 2003.

Jian Du, Brian Fix, James Glimm, Xicheng Jia, Xiaolin Li, Yunhua Li, and Lingling Wu. A simple package for front tracking. *J. Comp. Phys.*, 213:613–628, 2006.

B. Fix, J. Glimm, X. Li, Y. Li, X. Liu, R. Samulyak, and Z. Xu. A TSTT integrated FronTier code and its applications in computational fluid physics. *Journal of Physics: Conf. Series*, 16:471 – 475, 2005.

Y.A. Gorby. Microbial impacts on clay transformation and reactivity – controlled cultiviation: Approaches for debugging biogeochemical research. In *Minisymposia on Bioinformatics and Computational Biology*, June 23, 2004.

R. Ishizaki and et al. Two-dimensional simulation of pellet ablation with atomic processes. *Phys. Plasmas*, 11:4064–4080, 2004.

H. Johansen and P. Colella. A Cartesian grid embedded boundary method for Poisson's equation on irregular domains. *J. Comp. Phys*, 147:60–85, 1998.

X. F. Liu, E. George, W. Bo and J. Glimm. Turbulent Mixing with Physical Mass Diffusion. *Phys. Rev. E*, 73:056301-1–056301-8, 2006.

A. K. MacAulay. Geometrical, kinetic and atomic physics effects in a two dimensional time dependent simulation of ablating fuel pellets. *Nuclear Fusion*, 34:43–62, 1994.

P. Parks and R. J. Turnbull. Effect of transonic flow in ablation cloud on lifetime of a solid hydrogen pellet in a plasma. *Phys. Fluids*, 21:1735–1741, 1978.

R. Samulyak, T. Lu and P. Parks. A hydromagnetic simulation of pellet ablation in electrostatic approximation. *Nuclear Fusion*, 47:103-118, 2007.

R. Samulyak and Y. Prykarpatskyy. Richtmyer-Meshkov instability in liquid metal flows: influence of cavitation and magnetic fields. *Mathematics and Computers in Simulations*, 65:431–446, 2004.

M.S. Shephard, J.E. Flaherty, K.E. Jansen, X. Li, X.-J. Luo, N. Chevaugeon, J.-F. Remacle, M.W. Beall, and R.M. OBara. Adaptive mesh generation for curved domains. *J. for Applied Numerical Mathematics*, 53(2-3):251–271, 2005.

H.E. Trease. The virtual microbial cell simulator (VMCS): A computational simulation hierarchy for modeling the systems biology of microbial cells. *SIAM Conference on Computational Science and Engineering*, Minisymposia on Bioinformatics and Computational Biology, Feb. 10-13, 2002.

Z.L. Xu, M. Kim, T. Lu, W. Oh, J. Glimm, R. Samulyak, X.L. Li, and C. Tzanos. Discrete bubble modeling of unsteady cavitating flow. *International Journal for Multiscale Computational Engineering*, 4:601-616, 2006.